Supporting Information

Ultra-thin and Porous $MoSe_2$ Nanosheets: Facile Preparation and Enhanced Electrocatalytic Activity towards Hydrogen Evolution Reaction

Zhouyue Lei, Shengjie Xu and Peiyi Wu*

State Key Laboratory of Molecular Engineering of Polymers, Collaborative Innovation Center of Polymers and Polymer Composite Materials, Department of Macromolecular Science and Laboratory for Advanced Materials, Fudan University, Shanghai 200433, China.

Experimental Section

Materials: $MoSe_2$ were purchased from Alfa Aesar Corporation, IPA and H_2O_2 (30 wt%) were supplied from Sinopharm Chemical Reagent Co. Ltd. Nafion solution (5 wt%) was purchased from Sigma–Aldrich. All reagents were of analytical grade and used without further purification. N_2 with a purity of 99.9% was purchased from Shanghai Jifu Gas Co. Ltd.

Preparation of porous $MoSe_2$ nanosheets: Ultra-thin and porous $MoSe_2$ nanosheets was prepared through a simple modified liqude exfoliation process. Typically, 1 g of bulk $MoSe_2$ flakes were dispersed in 100 mL of IPA with 2.5 vol% of H_2O_2 and then kept sonication for 5 h. In case of over oxdiztion, the supernatant was decanted to remove extra H_2O_2 and the precipitate was further dispersed in 100 mL of IPA and

kept sonication for another 3 h. Left to stand overnight or centrifuged at 4000 rpm to separate the centrifugate and supernatant, the ultra-thin and porous $MoSe_2$ nanosheets suspension was collected. Porous $MoSe_2$ nanosheet suspension was dried at 50 ^oC under vacuum to obtain the solid samples for further use. For comparation, the ordinary $MoSe_2$ nanosheets were prepared according to our previous work,[1] in which 1 g of $MoSe_2$ powder and 100 mL of pure IPA or NMP were kept sonication for 8~10 h. Then the dispersion was kept undisturbed overnight and the few-layer $MoSe_2$ nanosheets suspension was collected.

Electrochemical measurements: Electrochemical measurements were carried out with a computer-controlled potentiostat (CHI660D) in a standard three-electrode cell using a platinum wire as a counter electrode and Ag/AgCl (in 3 M KCl solution) as a reference electrode. 1 mg of sample was first ultrasonically dispersed in 300 μl of Nafion solution (5 wt%), afterwards, the suspension (~10 μl) was attached onto a glass carbon (GC) electrode as a working electrode. For comparison, the few-layer $MoSe_2$ nanosheets and commercial Pt (20 wt% Pt/C) catalysts were also measured as reported in our previous work.[1-3] Besides, the EIS measurements were also performed at η = 0.44 V ranging from 10^6 to 0.1 Hz with an alternating current voltage of 10 mV.[4] CV curves were obtained on a potential range of 0.15-0.25 V vs RHE as reported before.[5]

Characterization: AFM images were obtained by using a Multimode V8 with the tapping mode after the samples were deposited on a freshly cleaved mica surface by spin coating. The HRTEM images were recorded on a JEOL JEM2011 at 200 kV.

XPS spectra were acquired by a RBD upgraded PHI-5000C ESCA system (Perkin Elmer) with Mg Ka radiation (hv = 1253.6 eV). XRD results were acquired by a D8 ADVANCE and DAVINCI.DESIGN (Bruker) X'pert diffractometer with Cu Kα radiation. Raman spectra were provided by XploRA Laser Raman spectrometer equipped with 638 nm helium/neon laser and CCD detector. The UV-vis spectra were recorded on a Hitachi U-2910 spectrophotometer. FESEM observations were performed on Zeiss Ultra 55 with energy dispersive X-ray spectroscopy (EDX).

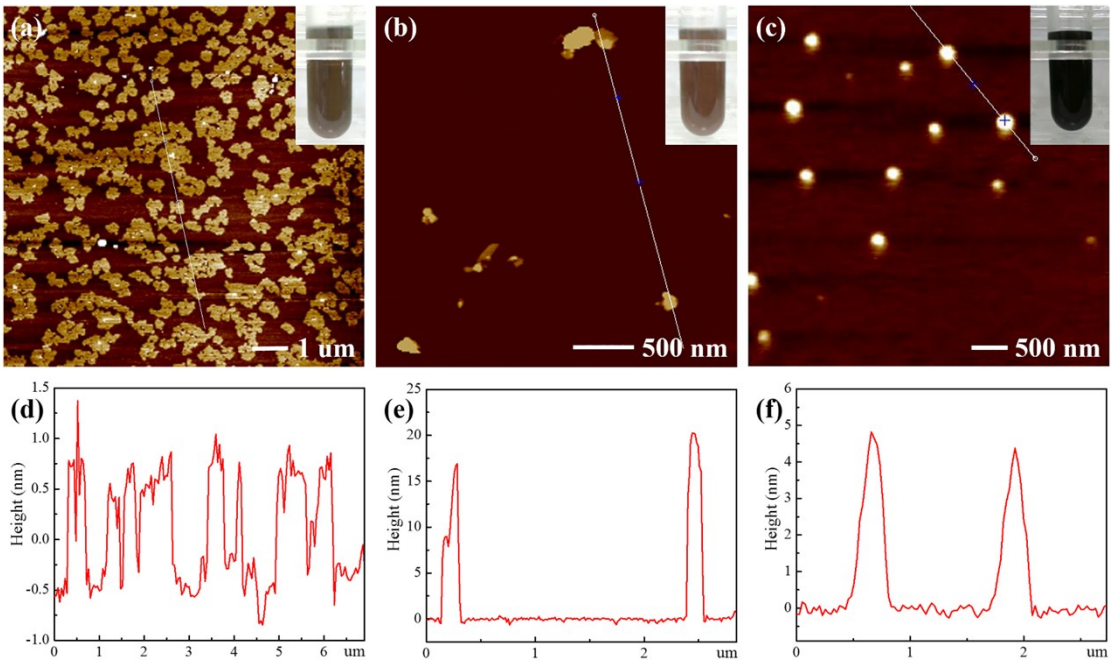

Fig. S1 AFM images of (a) ultra-thin and porous $MoSe_2$ nanosheets, (b) $MoSe_2$ nanosheets prepared in IPA and (c) $MoSe_2$ nanosheets prepared in NMP. Insets correspond to their nanosheet suspension.

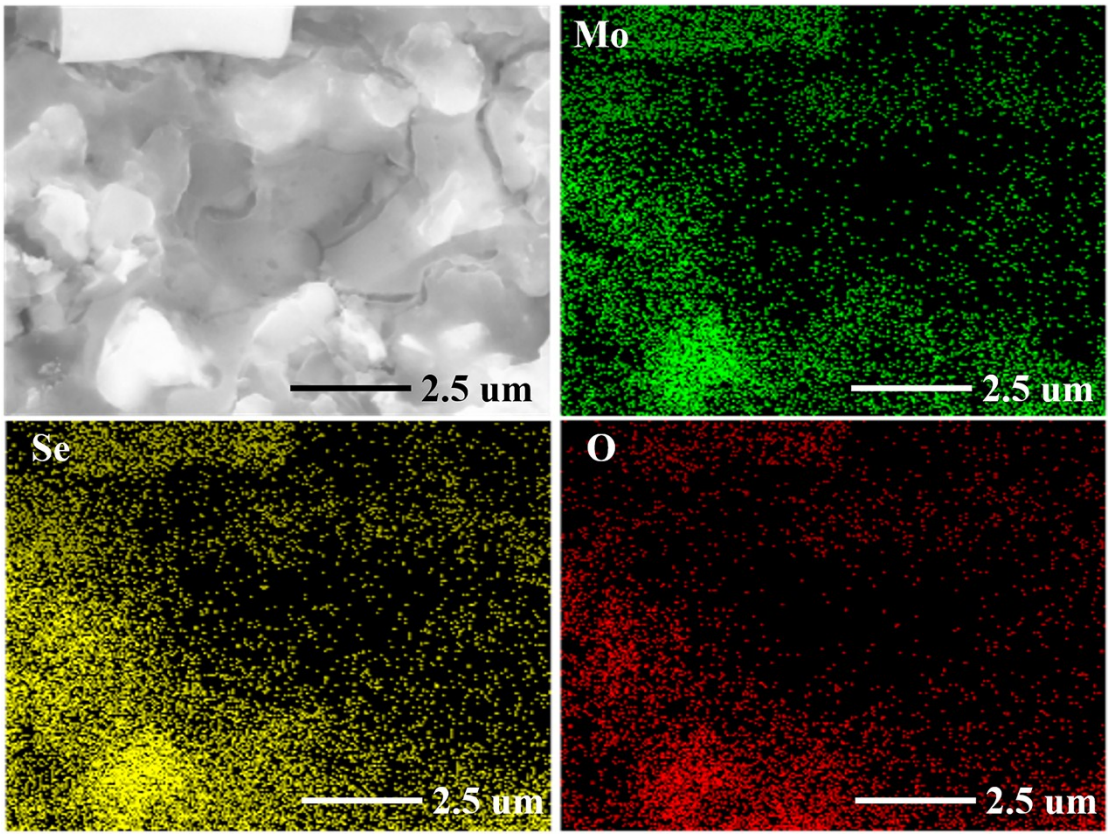

Fig. S2 FESEM image, element mapping images of ultra-thin and porous $MoSe_2$ nanosheets.

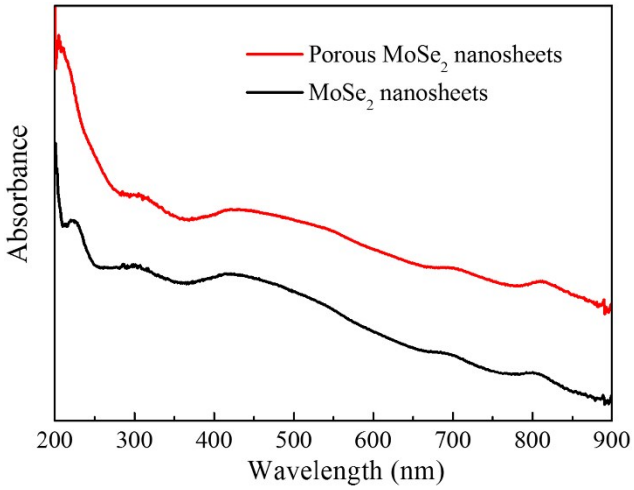

Fig. S3 UV-vis spectra of the ultra-thin and porous $MoSe_2$ nanosheets and $MoSe_2$ nanosheets prepared in IPA.

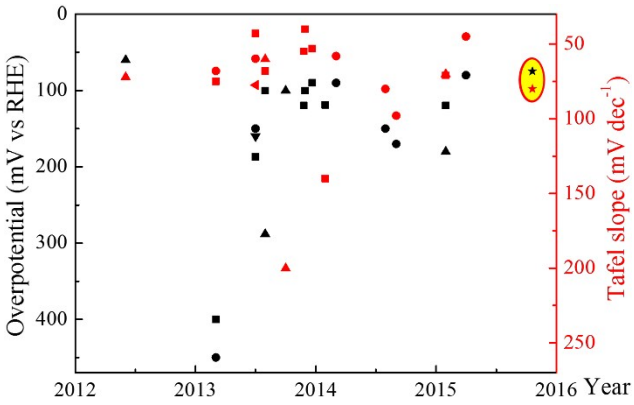

Fig. S4 A summary of HER performances of the reported TMD nanosheets and the cureent work (the star symbols). The square symbols correspond to the MoS_2 nanosheets, the circular symbols correspond to the $MoSe_2$ nanosheets, the regular triangles correspond to the WS_2 nanosheets and the inverted triangles correspond to the WSe_2 nanosheets.

Table S1 A summary of HER performances of the reported MoS_2 nanosheets (films).

	MoS_2	Overpotential (mV vs RHE)	Tafel slope (mV dec^{-1})	References
2013.2	Vertically aligned MoS_2 films	400	75	6
2013.6	Exfoliated metallic MoS_2 nanosheets	187	43	7
2013.7	MoS_2 nanosheets	100	68	8
2013.11	Oxygen-incorporated MoS_2 ultrathin nanosheets	120	55	9
2013.11	Conducting MoS_2 nanosheets	100	40	4
2013.12	Ultrathin MoS_2 nanoplates	90	53	10
2014.1	Single-layer MoS_2 nanosheets	119	140	11
2015.1	MoS_2 nanosheets decorated with	120	71	12

	MoS_2 quantum dots			

Table S2 A summary of HER performances of the reported $MoSe_2$ nanosheets (films).

$MoSe_2$		Overpotential (mV vs RHE)	Tafel slope (mV dec^{-1})	Refer-ences
2013.2	Vertically aligned $MoSe_2$ films	450	68	[6]
2013.6	$MoSe_2$ nanofilms with molecular layers perpendicular to the curved and rough surfaces.	150	59.8	[13]
2014.2	Ultrathin S-doped $MoSe_2$ nanosheets	90	58	[14]
2014.7	Macroporous $MoSe_2$ films	150	80	[15]
2014.8	Mo-rich hierarchical ultrathin $MoSe_{2-x}$ nanosheets	170	98	[16]
2015.3	$MoS_{2(1-x)}$ Se_{2x} alloy nanoflakes	80	45	[17]

Table S3 A summary of HER performances of the reported WS_2 nanosheets (films).

WS_2		Overpotential (mV vs RHE)	Tafel slope (mV dec^{-1})	Refer-ences
2012.5	WS_2 nanosheets	60	72	[18]
2013.7	Strained chemically exfoliated WS_2 nanosheets	288	60	[19]

2013.9	WS_2 nanoflakes	100	200	20
2015.1	WS_2 nanosheets decorated with WS_2 quantum dots	180	70	12

Table S4 A summary of HER performances of the reported WSe_2 nanosheets (films).

	WSe_2	Overpotential (mV vs RHE)	Tafel slope (mV dec^{-1})	Refer-ences
2013.6	WSe_2 nanofilms with molecular layers perpendicular to the curved and rough surfaces.	160	77.4	13

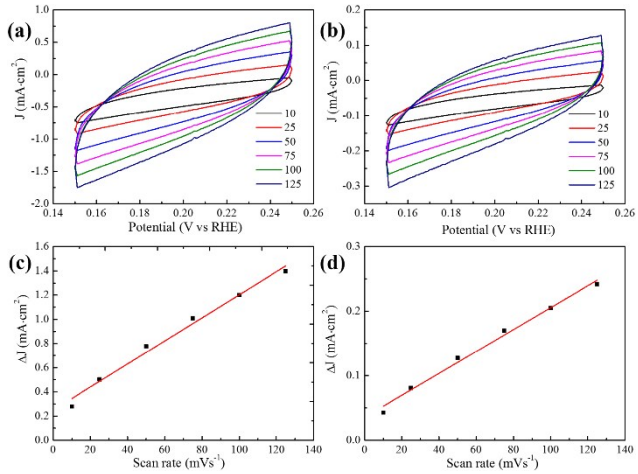

Fig. S5 Typical CV curves (top row) and corresponding differences in the current density at 0.2 V plotted against scan rate (bottom row). (a) and (c) are corresponding to the ultra-thin and porous $MoSe_2$ nanosheets, (b) and (d) are corresponding to the few-layer $MoSe_2$ nanosheets exfoliated in NMP.

Table S5 Summary of C_{dl} and electrochemical active surface area values of the ultra-thin and porous $MoSe_2$ nanosheets and few-layer $MoSe_2$ nanosheets exfoliated in NMP.

Samples	C_{dl} (mF cm^{-2})	Electrochemical active surface area
Porous $MoSe_2$ nanosheets	4.77	79
$MoSe_2$ nanosheets exfoliated in NMP	0.85	14

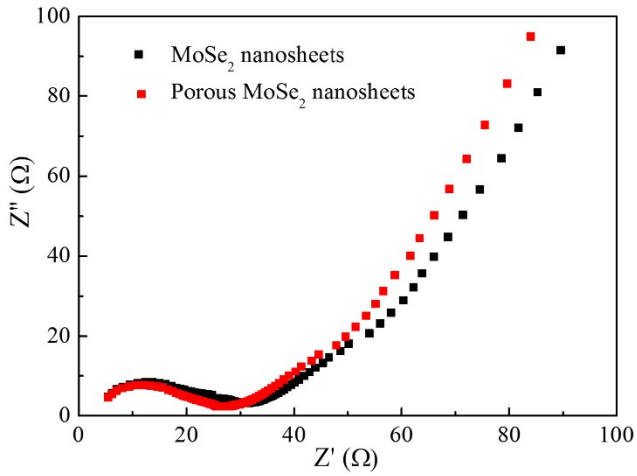

Fig. S6 Nyquist plots of ultra-thin and porous $MoSe_2$ nanosheets and few-layer $MoSe_2$ nanosheets prepared in NMP.

REFERENCES

1. S. Xu, Z. Lei and P. Wu, *J. Mater. Chem. A*, 2015, **3**, 16337-16347.

2. S. Xu, L. Yong and P. Wu, *Acs Appl. Mater. Inter.* , 2013, **5**, 654-662.

3. S. Xu, D. Li and P. Wu, *Adv. Funct. Mater.*, 2015, ***25***, 1127-1136.

4. D. Voiry, M. Salehi, R. Silva, T. Fujita, M. Chen, T. Asefa, V. B. Shenoy, G. Eda and M. Chhowalla, *Nano Lett.*, **2013**, ***13***, 6222-6227.

5. Y. Zheng, Y. Jiao, L. H. Li, T. Xing, Y. Chen, M. Jaroniec and S. Z. Qiao, *ACS Nano*, 2014, ***8***, 5290-5296.

6. D. Kong, H. Wang, J. J. Cha, M. Pasta, K. J. Koski, J. Yao and Y. Cui, *Nano Lett.*, 2013, **13**, 1341-1347.

7. M. A. Lukowski, A. S. Daniel, F. Meng, A. Forticaux, L. Li and S. Jin, *J. Am. Chem. Soc.*, 2013, **135**, 10274-10277.

8. Z. Wu, B. Fang, Z. Wang, C. Wang, Z. Liu, F. Liu, W. Wang, A. Alfantazi, D.

Wang and D. P. Wilkinson, *ACS Catalysis*, 2013, **3**, 2101-2107.

9. J. Xie, J. Zhang, S. Li, F. Grote, X. Zhang, H. Zhang, R. Wang, Y. Lei, B. Pan and Y. Xie, *J. Am. Chem. Soc.*, 2013, **135**, 17881-17888.

10. Y. Yan, B. Xia, X. Ge, Z. Liu, J.-Y. Wang and X. Wang, *Acs Appl. Mater. Inter.*, 2013, **5**, 12794-12798.

11. Y. Yu, S.-Y. Huang, Y. Li, S. N. Steinmann, W. Yang and L. Cao, *Nano Lett.*, 2014, **14**, 553-558.

12. S. Xu, D. Li and P. Wu, *Adv. Funct. Mater.*, 2015, **25**, 1127-1136.

13. H. Wang, D. Kong, P. Johanes, J. J. Cha, G. Zheng, K. Yan, N. Liu and Y. Cui, *Nano Letters*, 2013, **13**, 3426-3433.

14. C. Xu, S. Peng, C. Tan, H. Ang, H. Tan, H. Zhang and Q. Yan, *J. Mater. Chem. A*, 2014, **2**, 5597-5601.

15. F. H. Saadi, A. I. Carim, J. M. Velazquez, J. H. Baricuatro, C. C. L. McCrory, M. P. Soriaga and N. S. Lewis, *ACS Catalysis*, 2014, **4**, 2866-2873.

16. X. Zhou, J. Jiang, T. Ding, J. Zhang, B. Pan, J. Zuo and Q. Yang, *Nanoscale*, 2014, **6**, 11046-11051.

17. Q. Gong, L. Cheng, C. Liu, M. Zhang, Q. Feng, H. Ye, M. Zeng, L. Xie, Z. Liu and Y. Li, *ACS Catalysis*, 2015, **5**, 2213-2219.

18. Z. Wu, B. Fang, A. Bonakdarpour, A. Sun, D. P. Wilkinson and D. Wang, *Appl. Catal. B-Environ.*, 2012, **125**, 59-66.

19. D. Voiry, H. Yamaguchi, J. Li, R. Silva, D. C. B. Alves, T. Fujita, M. Chen, T. Asefa, V. B. Shenoy, G. Eda and M. Chhowalla, *Nat. Mater.*, 2013, **12**, 850-

855.

20. C. Choi, J. Feng, Y. Li, J. Wu, A. Zak, R. Tenne and H. Dai, *Nano Res.*, 2013, **6**, 921-928.